

# Lipid Profiling by Multiple Precursor and Neutral Loss Scanning Driven by the Data-Dependent Acquisition

Dominik Schwudke,<sup>†</sup> Jeffrey Oegema,<sup>‡</sup> Lyle Burton,<sup>§</sup> Eugeni Entchev,<sup>†</sup> J. Thomas Hannich,<sup>†</sup> Christer S. Ejsing,<sup>†</sup> Teymuraz Kurzchalia,<sup>†</sup> and Andrej Shevchenko<sup>\*,†</sup>

MPI of Molecular Cell Biology and Genetics, Pfotenhauerstrasse 108, 01307 Dresden, Germany, Scionics Computer Innovation GmbH, Tatzberg 47-51, 01307 Dresden, Germany, and MDS Sciex, Concord, 71 Four Valley Drive, L4K 4V8 Concord, Canada

**Data-dependent acquisition of MS/MS spectra from lipid precursors enables to emulate the simultaneous acquisition of an unlimited number of precursor and neutral loss scans in a single analysis. This approach takes full advantage of rich fragment patterns in tandem mass spectra of lipids and enables their profiling by complex (Boolean) scans, in which masses of several fragment ions are considered within a single logical framework. No separation of lipids is required, and the accuracy of identification and quantification is not compromised, compared to conventional precursor and neutral loss scanning.**

The full complement of individual molecular species of lipids in the cell has been termed as a lipidome.<sup>1,2</sup> Lipids are exceptionally diverse in their structural, chemical, and physical properties, and a large number of lipid species of various classes is present in the cell membranes. For example, a pool of phosphatidylcholines in a relatively simply organized red blood cell membrane comprises more than 100 molecular species<sup>3</sup> with the total number of glycerophospholipid species likely exceeding several hundred.<sup>4</sup> The structural heterogeneity of lipids and, consequently, the variability of their physical properties, enables the cell to form lateral microdomains,<sup>5</sup> to engage and cluster membrane proteins,<sup>6</sup> to polarize the cell surface,<sup>7</sup> and to adjust the cell shape without compromising the overall integrity of the membrane.<sup>8,9</sup>

Compositional differences between various membranes, membrane compartments, or microdomains are often quantitative,

rather than qualitative.<sup>10</sup> To understand how the altered lipid composition impinges over a wide gamut of molecular mechanisms of intracellular processes, lipidomic analytical technologies have been developed for the detection and quantification of hundreds of individual lipid species of various classes in minute amounts of lipid extracts. Electrospray ionization mass spectrometry has proved to be a powerful tool for lipid analysis (reviewed in refs 1, 11, and 12) and is typically used in two major ways. Lipid extracts can be separated on a chromatographic column and eluted species identified and quantified by on-line mass spectrometry.<sup>13–15</sup> LC–MS or LC–MS/MS detection increases the dynamic range and, likely, reduces the signal suppression. However, since species from different classes usually co-elute and the baseline separation of individual species is practically impossible, their unequivocal detection is difficult. Also, the column memory and biased recovery of lipids should be carefully accounted for, especially if analyzed samples differ strongly in their abundance, lipid composition, or both,<sup>13,16</sup> and the technique does not lend itself to high-throughput screens since separating complex lipid mixtures by HPLC is time-consuming.

Alternatively, the unseparated lipid extracts could be infused directly into a mass spectrometer and lipid species identified and quantified by specific precursor ion scans (PIS) and neutral loss scans (NLS),<sup>17–19</sup> which are typical operation modes of triple quadrupole mass spectrometers. Because of the relatively low scanning speed, the sensitivity improves with extending the analysis time at the uncompromised ionization efficiency. There-

\* Corresponding author: (e-mail) shevchenko@mpi-cbg.de.

<sup>†</sup> MPI of Molecular Cell Biology and Genetics.

<sup>‡</sup> Scionics Computer Innovation GmbH.

<sup>§</sup> MDS Sciex.

(1) Han, X.; Gross, R. W. *Mass Spectrom. Rev.* **2005**, *24*, 367–412.

(2) Han, X.; Gross, R. W. *J. Lipid Res.* **2003**, *44*, 1071–1079.

(3) Ekroos, K.; Ejsing, C. S.; Bahr, U.; Karas, M.; Simons, K.; Shevchenko, A. *J. Lipid Res.* **2003**, *44*, 2181–2192.

(4) Connor, W. E.; Lin, D. S.; Thomas, G.; Ey, F.; DeLoughery, T.; Zhu, N. J. *Lipid Res.* **1997**, *38*, 2516–2528.

(5) Simons, K.; Ikonen, E. *Nature* **1997**, *387*, 569–572.

(6) Simons, K.; Toomre, D. *Nat. Rev. Mol. Cell Biol.* **2000**, *1*, 31–39.

(7) Bagnat, M.; Simons, K. *Proc. Natl. Acad. Sci. U.S.A.* **2002**, *99*, 14183–14188.

(8) Martin, S. W.; Konopka, J. B. *Eukaryotic Cell* **2004**, *3*, 675–684.

(9) Leidy, C.; Goussset, K.; Ricker, J.; Walkers, W. F.; Tsvetkova, N. M.; Tablin, F.; Crowe, J. H. *Cell Biochem. Biophys.* **2004**, *40*, 123–148.

(10) Wenk, M. R. *Nat. Rev. Drug Discovery* **2005**, *4*, 594–610.

(11) Pulfer, M.; Murphy, R. C. *Mass Spectrom. Rev.* **2003**, *22*, 332–364.

(12) Griffiths, W. J. *Mass Spectrom. Rev.* **2003**, *22*, 81–152.

(13) Hermansson, M.; Uphoff, A.; Kakela, R.; Somerharju, P. *Anal. Chem.* **2005**, *77*, 2166–2175.

(14) Taguchi, R.; Hayakawa, J.; Takeuchi, Y.; Ishida, M. *J. Mass Spectrom.* **2000**, *35*, 953–966.

(15) Houjou, T.; Yamatani, K.; Imagawa, M.; Shimizu, T.; Taguchi, R. *Rapid Commun. Mass Spectrom.* **2005**, *19*, 654–666.

(16) DeLong, C. J.; Baker, P. R. S.; Samuel, M.; Cui, Z.; Thomas, M. J. *J. Lipid Res.* **2001**, *42*, 1959–1968.

(17) Brugger, B.; Erben, G.; Sandhoff, R.; Wieland, F. T.; Lehmann, W. D. *Proc. Natl. Acad. Sci. U.S.A.* **1997**, *94*, 2339–2344.

(18) Wenk, M. R.; Lucast, L.; Di Paolo, G.; Romanelli, A. J.; Suchy, S. F.; Nussbaum, R. L.; Cline, G. W.; Shulman, G. I.; McMurray, W.; De Camilli, P. *Nat. Biotechnol.* **2003**, *21*, 813–817.

(19) Liebisch, G.; Lieser, B.; Rathenberg, J.; Drobnik, W.; Schmitz, G. *Biochim. Biophys. Acta* **2004**, *1686*, 108–117.

fore, in lipidomics, triple quadrupole machines are typically operated with nanoelectrospray ion sources.<sup>17</sup> Neutral or poorly ionizable lipids could be analyzed as adducts with lithium or ammonia cations,<sup>20–22</sup> chloride or acetate anions,<sup>3</sup> or subjected to chemical derivatization<sup>23,24</sup> to localize the net charge on their molecules. The dynamic range of detection could be further improved by “in-source” separation,<sup>25</sup> in which, by varying electrospray ionization parameters and the composition of an electrosprayed analyte, preferential ionization of certain lipid class(es) is achieved.

While very sensitive, and sufficiently specific, precursor ion scanning on triple quadrupole instruments is still an inherently low-throughput approach. Only a single precursor or neutral loss scan can be performed at a time, and the analysis must be repeated to profile multiple classes of lipids. Another, usually less recognized, limitation is the relatively low specificity of the fragment ion selection by the Q3 analytical quadrupole. For better sensitivity, it is typically operated under the low mass resolution settings, and therefore,  $m/z$  of the fragment ion is selected within the range of 1–2 Da.

Multiple precursor ion scanning implemented on a hybrid quadrupole time-of-flight mass spectrometer (reviewed in ref 26) addressed these problems and opened up novel analytical opportunities in lipidomics.<sup>27</sup> In Q(q)TOF instruments, precursor ions are also selected by the Q1 analytical quadrupole. The entire pool of fragment ions, rendered from the precursor ion in the collision cell, is detected by a non-scanning TOF analyzer, and therefore, virtually unlimited number of precursor ion scans can be performed simultaneously. Furthermore, the high mass resolution of the TOF analyzer does not compromise the detection sensitivity, and therefore,  $m/z$  of fragment ions are typically selected within the range of less than 0.2 Da, thus drastically increasing the specificity of precursor ion scanning and reducing chemical noise. Upon low-energy collision-induced fragmentation, molecular anions of glycerophospholipids produce abundant acyl anions of their fatty acid moieties.  $M/z$  of acyl anions of a large number of fatty acids, which may or may not be present in analyzed lipids, could be selected and the corresponding precursor ion spectra acquired in parallel—this approach was termed FAS for fatty acid scanning.<sup>3,27</sup> Accurate selection of  $m/z$  of acyl anions of fatty acids of interest enhanced the dynamic range of the analysis and enabled the identification of very low abundant molecular species from various classes of glycerophospholipids comprising the moieties of specific fatty acids.<sup>28</sup> Being both specific and comprehensive, the method provided a global overview of changes in the fatty acid composition of lipids, enriched in certain lipid fractions or membrane domains.<sup>29</sup>

The systematic use of multiple precursor ion scanning in lipidomics projects also revealed its inherent limitations. Although simultaneous acquisition of multiple precursor ion spectra is possible, parallel acquisition of multiple neutral loss spectra is not. This hampers class-specific profiling of several glycerophospholipid classes, such as phosphatidylethanolamines (PEs), phosphatidylserines (PSs), and triacylglycerols (TAGs), among others, whose fragmentation does not render abundant ions of headgroup fragments. The acquired pool of precursor ion spectra does not lend itself to subsequent reprocessing, such as, for example, profiling for another fragment ion or neutral loss or for a pair of fragments with complementary masses. Accurate quantification of lipid species by precursor ion scanning requires the maintenance of better than the unit resolution of the analytical quadrupole Q1 and, therefore, limits the efficiency of ion transmission at the relatively high (>1000 Da)  $m/z$  range. This compromises the sensitivity of detection of several lipid classes, such as phosphatidylinositol phosphates.<sup>18</sup>

Here we describe a method that effectively amends these deficiencies. Data-dependent (also termed as information-dependent) acquisition of full MS/MS spectra from all detectable precursor ions enabled the emulation of the simultaneous acquisition of an unlimited number of precursor and neutral loss scans in a single analysis. No separation of lipids was required, and the accuracy of identification and quantification was not compromised, compared to conventional precursor and neutral loss scans. By combining a Q(q)TOF mass spectrometer with an automated nanoelectrospray chip-based ion source,<sup>30</sup> the approach lends itself to full automation and high-throughput lipidomic analysis.

## MATERIALS AND METHODS

**Materials and Lipid Standards.** Synthetic lipid standards and purified preparations of PC, PE, and phosphatidylinositol (PI) from bovine brain and heart were purchased from Avanti Polar Lipids, Inc. (Alabaster, AL), Sigma-Aldrich Chemie GmbH (Munich, Germany), and Echelon Research Laboratories, Inc. (Salt Lake City, UT). Chloroform, methanol, and ammonium acetate were liquid chromatography grade and purchased from Fluka (Buchs SG, Switzerland).

**Sample Preparation for Mass Spectrometric Analysis.** Stock solutions of lipid standards were prepared in different concentrations and molar ratios in  $\text{CHCl}_3/\text{MeOH}$  1:2 (v/v) containing 5 mM ammonium acetate. Prior to the analysis, samples were vortexed thoroughly and centrifuged for 5 min at 14 000 rpm on a Minispin centrifuge (Eppendorf, Hamburg, Germany). Samples were loaded onto 96-well plates and sealed with aluminum foil.

**Isolation of Lipids from *Caenorhabditis elegans* Worms.** Wild type *C. elegans* Bristol N2 worms were grown at 20 °C on NGM agar plates according to a standard procedure.<sup>31</sup> Typically, for the lipid extraction, ~200  $\mu\text{L}$  of pelleted worms was used. After three cycles of freezing in liquid nitrogen and thawing in an ultrasound bath, phospholipids were extracted as described in ref

(20) Hsu, F. F.; Turk, J. J. *Mass Spectrom.* **2000**, *35*, 595–606.

(21) Hsu, F. F.; Turk, J. J. *Am. Soc. Mass Spectrom.* **1999**, *10*, 587–599.

(22) Han, X.; Gross, R. W. *Anal. Biochem.* **2001**, *295*, 88–100.

(23) Sandhoff, R.; Brugger, B.; Jeckel, D.; Lehmann, W. D.; Wieland, F. T. *J. Lipid Res.* **1999**, *40*, 126–132.

(24) Han, X.; Yang, K.; Cheng, H.; Fikes, K.; Gross, R. W. *J. Lipid Res.* In press.

(25) Han, X.; Yang, J.; Cheng, H.; Ye, H.; Gross, R. W. *Anal. Biochem.* **2004**, *330*, 317–331.

(26) Chernushevich, I.; Loboda, A.; Thomson, B. J. *Mass Spectrom.* **2001**, *36*, 849–865.

(27) Ekroos, K.; Chernushevich, I. V.; Simons, K.; Shevchenko, A. *Anal. Chem.* **2002**, *74*, 941–949.

(28) Kuerschner, L.; Ejsing, C. S.; Ekroos, K.; Shevchenko, A.; Anderson, K. I.; Thiele, C. *Nat. Methods* **2005**, *2*, 39–45.

(29) Schuck, S.; Honsho, M.; Ekroos, K.; Shevchenko, A.; Simons, K. *Proc. Natl. Acad. Sci. U.S.A.* **2003**, *100*, 5795–5800.

(30) Kameoka, J.; Craighead, H. G.; Zhang, H.; Henion, J. *Anal. Chem.* **2001**, *73*, 1935–1941.

(31) Brenner, S. *Genetics* **1974**, *77*, 71–94.

32 and neutral lipids as described in ref 33. TAGs were isolated by a two-dimensional TLC on silica 60 F<sub>254</sub> 20 × 20 cm plates (Merck, Darmstadt, Germany) with the first migration in chloroform/methanol (24:1) and the second migration in *n*-hexane/diethyl ether: acetic acid (7:3:0.1). The *C. elegans* TAG spot was identified by a standard. The spot was scraped from the plate and TAGs were recovered from silica gel by the extraction according to Folch et al.<sup>34</sup>

**Mass Spectrometric Analysis.** The analysis was performed on a modified QSTAR Pulsar *i* quadrupole time-of-flight mass spectrometer (MDS Sciex, Concord, Canada) equipped with an automated nanospray chip ion source NanoMate HD (Advion BioSciences, Ithaca, NY). Ionization voltage was set to 1.05 kV, gas pressure to 0.1 psi and the source was controlled by Chipsoft 6.3.2 software (Advion BioSciences Ltd.). Lipid extracts were infused at the flow rate of ~250 nL/min. A typical sample volume of 10 μL allowed 40 min of stable electrospray time. The spraying stability was monitored by the total ion count (TIC) signal reported from survey TOF MS spectra. Samples with more than ±25% of the relative TIC variation throughout the analysis were discarded from the data set and reanalyzed later using a different nozzle.

In conventional precursor ion scanning mode, the analytical quadrupole Q1 was operated at unit resolution and 30 ms dwell time with step size of 0.2 Da. The collision energy offset was 45 eV, and *m/z* of fragment ions were selected within the range of 0.2 Da. Peak intensities were maintained below 750 counts/s to avoid saturation of the detector. Peak enhancement (trapping of fragment ions of the selected *m/z* in the collision cell) was applied according to the instructions of the manufacturer and was controlled by Analyst QS 1.1 software. Acquired spectra were interpreted and the detected species quantified by a prototype Lipid Profiler software (MDS Sciex, Concord, Canada).

Data-dependent acquisition (DDA) experiments were performed under the collision energy offset of 35 eV. A typical DDA cycle comprised the acquisition of a survey TOF MS spectrum (2 s) followed by two consecutive MS/MS experiments. In the first experiment, the analytical quadrupole Q1 was operated under the unit resolution settings and fragments were detected in the *m/z* range of 100–500 with acquisition time of 20 s. In the second experiment, Q1 was operated under the low mass resolution settings that allowed transmission of the entire isotopic cluster and fragments were detected in the *m/z* range of 500–700 with the acquisition time of 10 s. The same precursor was fragmented in both MS/MS experiments and then its *m/z* was excluded until the end of the analysis. Upon completing the cycle, the instrument started a new cycle, in which either the next precursor candidate was identified by considering the intensities of peaks detected at the survey TOF MS spectrum or (where indicated) the next precursor *m/z* was taken from an inclusion list. Because of the similarity of the elemental composition of glycerophospholipids, *m/z* of their species are isobaric and distributed in slots spaced by 2 Da. Therefore, a single inclusion list was compiled for analyzing all glycerophospholipid precursor ions in the positive

ion mode. DDA-controlling software (Analyst QS 1.1) identified precursor ion candidates within the *m/z* window of 0.2 Da centered at the *m/z* taken from the inclusion list. Since the size of inclusion lists used by Analyst QS 1.1 was limited to 100 entries, precursors within a range of *m/z* 690–890 for glycerophospholipids, and a range of *m/z* 790–990 for TAGs, were analyzed. Acquired MS/MS spectra were exported as files in dta format by Analyst QS 1.1. All data files acquired in the same analysis were collected into a single dataset folder.

**Interpretation of DDA Experiments** was performed using the dedicated software LipidInspector developed by Scionics Computer Innovations GmbH (Dresden, Germany). LipidInspector is a software package developed in the Python programming language that uses the wxPython GUI toolkit, a wrapper of the wxWidgets C++ libraries, to provide a rich and cross-platform client. To date LipidInspector has been tested on Windows 2000, Windows XP, and Linux platforms and is available upon request.

The LipidInspector imported multiple dataset folders containing dta files. The first line of each dta file contained the precursor mass and the charge, followed by a peak list of centroided *m/z* and intensities of fragments detected in the MS/MS experiment. Depending on the acquisition mode polarity, collision activation of molecular ions of glycerophospholipids rendered fragments of headgroups, fatty acid moieties, or both as ions or neutrals. While examining dta files, the LipidInspector used the list of *m/z* of these specific fragments and neutral losses (provided in the Supporting Information) or identified fragments whose *m/z* met certain predefined selection criteria. In each dta file, the LipidInspector identified the fragment ions whose *m/z* matched, within the specified mass tolerance, either the *m/z* or *m/z* differences from the list and, hence, determined the lipid class of the fragmented precursor. We note here that *m/z* of precursors were either determined in full TOF MS survey scans or in survey scans restricted to 0.2-Da window around *m/z* from the inclusion list, rather than taken from the residual precursor peak detectable in the MS/MS spectrum. The LipidInspector reported the intensities of matched peaks for the subsequent quantitative analysis. From the exact *m/z* of each identified precursor, the software calculated the total number of carbon atoms and double bonds in its fatty acid moieties. From each dataset folder, species identified in all dta files, along with the intensities of corresponding peaks, were exported as a tab-delimited text file, which could be directly opened by Microsoft Excel. Isotopic correction of peak intensities was implemented as described by Han and Gross.<sup>1</sup>

## RESULTS AND DISCUSSION

**Work Flow of DDA-Driven Lipid Profiling.** DDA of tandem mass spectra is routinely employed in LC–MS/MS analysis. DDA experiments typically combine scans of several types (MS, MS/MS, neutral loss, etc.) within a single acquisition cycle and are powered by real-time selection of plausible precursors for the subsequent MS<sup>*n*</sup> analysis.<sup>15,35</sup> In this work, we adjusted the DDA methodology for quantitative profiling of unseparated lipid mixtures (Figure 1).

Data-dependent acquisition proceeded in cycles, typically consisting of one rapid TOF MS survey scan followed by the

(32) Bligh, E. G.; Dyer, W. J. *Can. J. Biochem. Physiol.* **1959**, *37*, 911–917.

(33) Matyash, V.; Entchev, E. V.; Mende, F.; Wilsch-Brauninger, M.; Thiele, C.; Schmidt, A. W.; Knolker, H. J.; Ward, S.; Kurzchalia, T. V. *PLoS Biol.* **2004**, *2*, e280.

(34) Folch, J. M.; Lees, M.; Sloane-Stanley, G. H. *J. Biol. Chem.* **1957**, *226*, 497–509.

(35) Wang, C.; Kong, H.; Guan, Y.; Yang, J.; Gu, J.; Yang, S.; Xu, G. *Anal. Chem.* **2005**, *77*, 4108–4116.

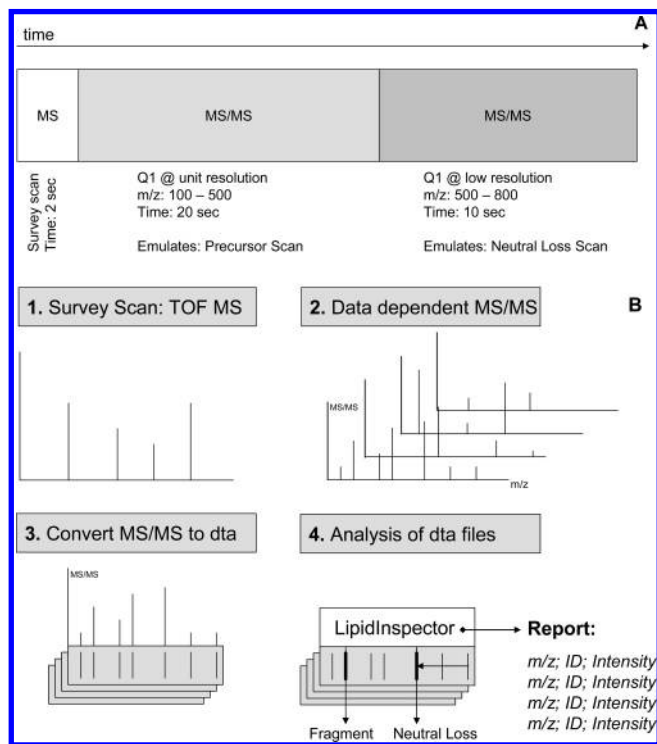


**Figure 1.** Acquisition cycle and workflow of DDA-driven lipid profiling. (A) The acquisition cycle consists of a 2 s survey scan and two consecutive MS/MS experiments; precursor ions are selected at the unit resolution of Q1 quadrupole for emulating precursor ion scans and low resolution for emulating neutral loss scans. (B) The workflow of a typical profiling experiment: (1) TOF MS survey scan identified  $m/z$  of prospective precursor ions; alternatively, they were taken from the inclusion list; (2) MS/MS spectra were acquired from the selected precursor(s); (3) all MS/MS spectra acquired in the same DDA experiment were exported into dta files composed of centroided  $m/z$  and intensities of fragment ions; (4) a batch of dta files was uploaded into the LipidInspector software, which identified fragment ions according to the specified selection criteria and determined the lipid class and sum composition of the fragmented precursor. Finally, the LipidInspector created a spreadsheet report with identified lipids along with the corresponding precursor  $m/z$  and intensities of the matched fragment ions for their subsequent quantification.

consecutive acquisition of two MS/MS spectra from the same selected precursor (Figure 1A). The first MS/MS spectrum was acquired under the unit mass resolution settings of the Q1 analytical quadrupole, covered fragments within low  $m/z$  region, and the abundance of the corresponding peaks was further used for emulating precursor ion scan(s). Lipid species of the same class, which only differ by one double bond and have the mass difference of 2 Da, yield the same headgroup fragment(s) and their quantification is compromised, if both precursors are co-selected by the quadrupole filter. Therefore, to emulate precursor ion scans quantitatively, the prospective precursors were selected by the Q1 analytical quadrupole under the unit resolution settings in order to minimize the contribution of a neighboring precursor to the abundance of the common fragment ion(s). The second consecutive MS/MS was acquired from the same precursor under the low mass resolution settings of the Q1 quadrupole, covered high  $m/z$  range of the spectrum and detected fragments rendered via the loss of neutral molecule(s) from the precursor ion. Because of the high mass resolution of the TOF analyzer, neutral loss

products originating from accidentally co-selected precursors were clearly distinguishable and less stringent mass resolution settings of the quadrupole were applied to enhance the ion transmission and improve sensitivity. Therefore, different time periods were set for the acquisition of the first and second MS/MS spectra. Depending on the analytical task and expected complexity of the analyte, the DDA cycle could be adjusted to either enhance the sensitivity or increase the number of fragmented precursors. This, however, did not alter the subsequent spectral interpretation routine.

The acquired MS/MS spectra were then exported as dta files and interpreted by the dedicated LipidInspector software. In each spectrum, the LipidInspector identified and reported the abundance of peaks, corresponding either to given mass differences between their  $m/z$  and  $m/z$  of the precursor ion (emulating neutral loss scans) or to the  $m/z$  of the given fragment ions (emulating precursor ion scans), or satisfying other, more complex, selection criteria (Boolean scans, explained below). By applying this procedure to the entire pool of MS/MS spectra, the software effectively emulated parallel acquisition of multiple precursor and neutral loss scans (Figure 1).

Because of the high sensitivity of the non-scanning TOF analyzer, a 2 s survey scan was sufficient to acquire good quality spectra over the full  $m/z$  range. We underscore that the DDA-driven quantification was performed via signals detected in MS/MS (rather than in TOF MS) mode and, therefore, was much less affected by possible saturation of the detection system and chemical noise. Even for lipid species present in the nanomolar concentration range, ion statistics of peaks detected in MS/MS spectra acquired for 20 and 10 s periods was sufficient for their robust quantification and the analysis of more than 55 precursors was completed in less than 30 min.

Compared to conventional precursor ion scanning, or neutral loss scanning, DDA used the analysis time more efficiently since tandem mass spectra were not acquired within  $m/z$  areas with no detectable precursor peaks. To encompass low-abundant species, a large inclusion list of prospective  $m/z$  could be compiled using brutto formulas of all species of interest, which may or may not be present in the sample. Since MS/MS spectra are almost free from chemical noise, low-abundant species, indistinguishable from background in survey TOF spectra, could still be reliably quantified.

**Validation of DDA-Driven Lipid Profiling.** DDA effectively emulated the parallel acquisition of multiple precursor and neutral loss spectra. Using standard lipid mixtures, we first determined whether the identified species and their relative intensities (here termed as a profile) obtained by conventional precursor scanning would match the profile deduced from a pool of MS/MS spectra by extracting the intensities of the same fragment ion. To this end, a preparation of phosphatidylcholines (PCs) from bovine heart was first analyzed in the positive ion mode by scanning for precursors of the characteristic headgroup fragment with  $m/z$  184.07 (+PIS  $m/z$  184.07). Peaks of PCs were identified by the Lipid Profiler and reported peak areas normalized to the area of the most abundant peak (Figure 2B). The same sample was further subjected to DDA-driven analysis, also in the positive ion mode. Areas of  $m/z$  184.07 peaks were extracted from all MS/MS spectra, normalized, and compared to the profile obtained by

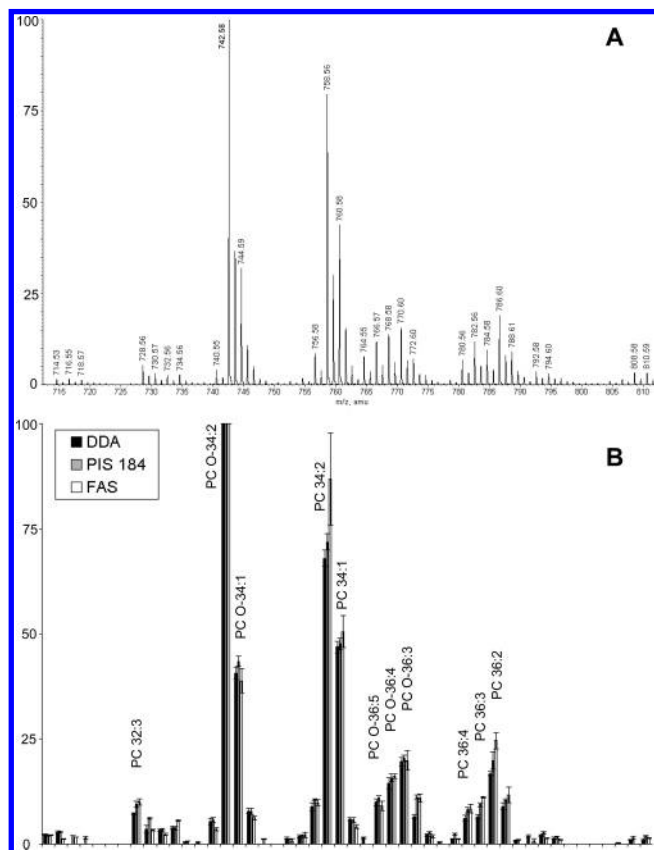


**Figure 2.** DDA-driven profiling of bovine heart PC extract with a total lipid concentration of 2 ng/ $\mu$ L. (A) +TOF MS survey scan; (B) normalized profile of PC species determined by DDA-driven +PIS  $m/z$  184.07 (filled bars), by conventional +PIS  $m/z$  184.07 (shaded bars), and by fatty acid scanning in the negative ion mode (unfilled bars), all normalized to the intensity of the most abundant PC O-34:2.

the “real” precursor ion scanning (Figure 2B). We concluded that both profiles agreed well.

The instrument was then switched to the negative ion mode and the same sample was subjected to FAS—multiple precursor ion scanning that uses  $m/z$  of acyl anions of common fatty acids as specific fragments.<sup>3,27</sup> For all PC species identified as adducts with acetate anions by the Lipid Profiler, the intensities of the acyl anions of both fatty acid moieties were summed up, normalized, and compared with the two +PIS  $m/z$  184.07 profiles (Figure 2B). All three independently acquired profiles were remarkably similar and encompassed all major peaks detectable in +TOF MS spectrum (Figure 2A). We therefore concluded that DDA-driven precursor ion scanning provided the same identification specificity and accuracy as did the established methods of conventional precursor ion scanning and FAS.

Q(q)TOF mass spectrometers cannot perform conventional neutral loss scanning. Therefore, to test whether the DDA-driven approach could adequately emulate neutral loss scanning, we compared the neutral loss scanning profile obtained *via* DDA with another profile produced from the same sample by the established method of conventional precursor ion scanning. PIs are readily detectable in the negative ion mode by precursor ion scanning for the headgroup fragment  $m/z$  241.01 or, in the positive ion mode, by the neutral loss of the headgroup plus ammonia  $\Delta m/z$  277.06 from their ammonium adducts.<sup>17,36</sup> We acquired the profile

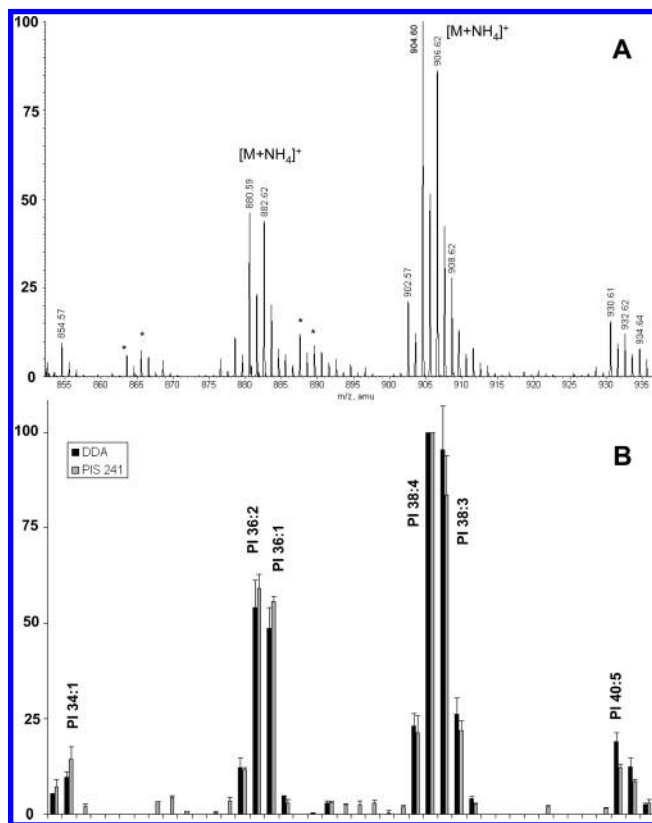


**Figure 3.** DDA-driven profiling of bovine brain PI extract with a total lipid concentration of 1.4 ng/ $\mu$ L. (A) +TOF MS survey scan; signals marked with asterisks are protonated PI species. (B) Normalized profile of PI species determined by DDA-driven +NLS  $\Delta m/z$  277.01 (filled bars) and by  $-PIS$   $m/z$  241.0 (shaded bars).

from the preparation of bovine brain PIs by  $-PIS$   $m/z$  241.01 and then compared it to the profile obtained by DDA-driven +NLS  $\Delta m/z$  277.06 (Figure 3B). Figure 3A presents +TOF MS spectrum of the mixture as a reference (note that PI species were mostly detected as ammonium adducts). Both methods independently and accurately identified all major PI species, and as judged by the comparison with +TOF MS profile, no abundant peaks were missed. The relative abundance of species identified by precursor ion scanning in the negative mode, and DDA-driven neutral loss scan profiling in the positive ion mode, were also in a good agreement. Although DDA-driven profiling was performed under the low mass resolution settings of the Q1 quadrupole, species that only differed by one double bond in a fatty acid moiety (PI 36:1 and PI 36:2; PI 38:5 and PI 38:4; PI 38:3 and PI 38:2, among others), were correctly distinguished and quantified. We note, however, that a few minor peaks detectable by +TOF MS were not interpreted by DDA-based neutral loss scanning since they represented protonated forms of abundant PIs (marked with asterisks in Figure 3A).

Taken together, the results presented in Figures 2 and 3 suggested that both DDA-driven precursor ion scanning and neutral loss scanning accurately and quantitatively determined profiles of the abundant lipid species and were in a good agreement with established methods of mass spectrometric lipid analysis.

#### Sensitivity and Accuracy of DDA-Driven Quantification of Lipids.

Using a mixture of 13 synthetic lipid standards of various

(36) Hsu, F. F.; Turk, J. J. *Am. Soc. Mass Spectrom.* **2000**, *11*, 986–999.

**Table 1. Limits of Quantification of Lipid Standards Determined by DDA-Driven Profiling**

lipid standard <sup>a</sup>	precursor ion, <i>m/z</i>	detected fragment ion or neutral loss, <i>m/z</i>	LOQ, <sup>b</sup> nM
	[M + H] <sup>+</sup>	neutral loss	
PE 18:0/18:2	744.5538	141.019	15
PE 20:4/20:4	788.5225	141.019	15
MMPE 18:1/18:1	758.5694	155.0347	15
DMPE 18:1/18:1	772.5851	169.0503	5
PS 18:0/18:2	788.5436	185.0089	15
PE-O-16:1p/20:4	724.5276	141.019	30
PE-O-16:1p/22:6	748.5276	141.019	35
		fragment ion	
DMPE 18:1/18:1	772.5851	170.0576	20
PC 16:0/22:6	806.5694	184.0733	15
SM 18:0	731.6062	184.0733	30
PE-O-16:1p/20:4	724.5276	364.2611/361.2737	20
PE-O-16:1p/22:6	748.5276	364.2611/385.2737	70
	[M + NH <sub>4</sub> ] <sup>+</sup>	neutral loss	
PA 17:0/17:0	694.5381	115.0034	30
PG 17:0/17:0	768.5749	189.0402	30
PI 16:0/16:0	828.5597	277.0562	50
TAG 16:0/16:0/16:0	824.7702	273.2667	15

<sup>a</sup> Phosphatidylethanolamine (PE), monomethylphosphatidylethanolamine (MMPE), dimethylphosphatidylethanolamine (DMPE), phosphatidylserine (PS), phosphatidylcholine (PC), sphingomyelin (SM), phosphatidic Acid (PA), phosphatidylglycerol (PG), phosphatidylinositol (PI), and triacylglycerol (TAG). <sup>b</sup> LOQ, limit of quantification is the lowest concentration of the analyte (in nM), which can be determined with the accuracy of  $\pm 3s$ , where  $s$  stands for the standard deviation of four independent measurements.

classes, we determined their limits of quantification and linearity of corresponding calibration curves in a series of dilution experiments (Table 1). Usually, the method sensitivity is estimated *via* the amount of injected sample, which enables us to detect the corresponding compound with a given signal-to-noise ratio. DDA-driven profiling relies on the abundance of fragment ions in MS/MS spectra, which are essentially noise-free. However, the accuracy of lipid quantification—the factor of paramount importance in lipidomics—mostly depends on ion statistics of quantified peaks, as well as on the reproducibility of the analysis conditions. Therefore, here we estimated the sensitivity of the analysis by determining the limit of quantification (LOQ), defined as the lowest concentration of the analyte that could be determined with the given accuracy. To this end, we performed four independent measurements for each of five dilutions of the lipid standard stock solution. LOQ was calculated as  $3s/B$ , where  $s$  stands for the standard deviation of four measurements at a single dilution and  $B$  stands for the slope of the corresponding calibration curve. LOQs of all analyzed lipid species were in the concentration range of 5–70 nM, depending on the lipid class and mode of detection, which suggested the high sensitivity of DDA-driven lipid profiling. Assuming that, in the profiling mode, two MS/MS spectra were acquired from each precursor ion for 30 s in total, the actual sample consumption was in the range of 0.6–9 fmol per analyzed lipid.

Calibration curves for all lipid species were linear within the concentration range of 40–1000 nM. Figure 4 presents two calibration plots for a dimethylphosphatidylethanolamine (DMPE) standard, which were obtained by DDA-driven +PIS  $m/z$  170.06 and +NLS  $\Delta m/z$  169.05. Although regression coefficients were similar for both plots, neutral loss detection reached the 4 $\times$  lower

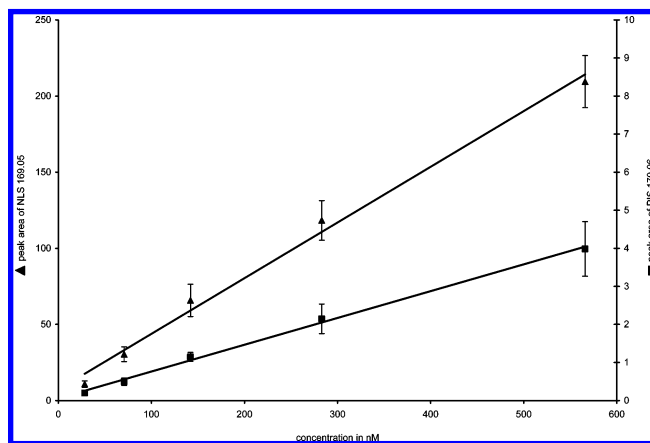


**Figure 4.** Calibration curves for the dimethylphosphatidylethanolamine synthetic standard (DMPE 18:1/18:1, see Table 1) obtained by DDA-driven +NLS  $\Delta m/z$  169.05 (filled triangles,  $r^2 = 0.993$ ) and +PIS  $m/z$  170.06 (filled squares,  $r^2 = 0.997$ ).

LOQ (Table 1). Note that neutral loss scanning was performed at the low mass resolution of Q1 analytical quadrupole, whereas precursor ion scanning required unit mass resolution. To estimate the effect of Q1 resolution on the detection sensitivity, we acquired tandem mass spectra from several precursors under the low-resolution and unit-resolution settings. Lower mass resolution enabled unperturbed transmission of precursor ions and increased the intensities of fragment ions, on average, by a factor of 3 (data not shown). This, in turn, improved the sensitivity and lowered corresponding LOQs, as was apparent for DMPE 18:1/18:1 (Table 1). Upon their collisional activation, ammonium adducts of lipids of several classes, such as phosphatidic acids (PAs), phosphatidylglycerols (PGs), and PIs, underwent neutral loss of their headgroups plus ammonia and allowed their profiling in the positive mode *via* DDA-driven neutral loss scanning (Table 1).

We note here that LOQs were most affected by the variability of spraying, rather than by the poor ion statistics of analyzed peaks, which might result in the substantial difference of LOQs of closely related compounds determined by the same method in a given series of measurements (Table 1). This, in principle, could be addressed by quantifying the species within the series of samples with similar lipid composition by the method of standard addition using the same nozzle of a nanospray chip.

**High Mass Accuracy Enhances the Specificity of DDA-Driven Neutral Loss Scanning.** Conventional neutral loss scanning on a triple quadrupole instrument takes advantage of accurate matching of the  $m/z$  difference between the precursor and the fragment ion. At the same time, the  $m/z$  of fragment ions are determined with relatively low accuracy because of the low mass resolution settings of the second analytical quadrupole Q3. However, in DDA-driven neutral loss scanning on a Q(q)TOF mass spectrometer, the  $m/z$  of fragment ions are determined with high accuracy, thus making the scans far more specific. For example, within the same lipid class, species with two ester bonds and species having one ester and one ether bond are isobaric if they differ by a single methylene group. Nevertheless, the difference of 0.0364 Da ( $m_O - m_{CH_4}$ ) between their exact masses could be confidently determined in MS/MS mode on a Q(q)TOF. Here we demonstrate that DDA-driven neutral loss scanning, together with the accurate determination of  $m/z$  of the fragments,

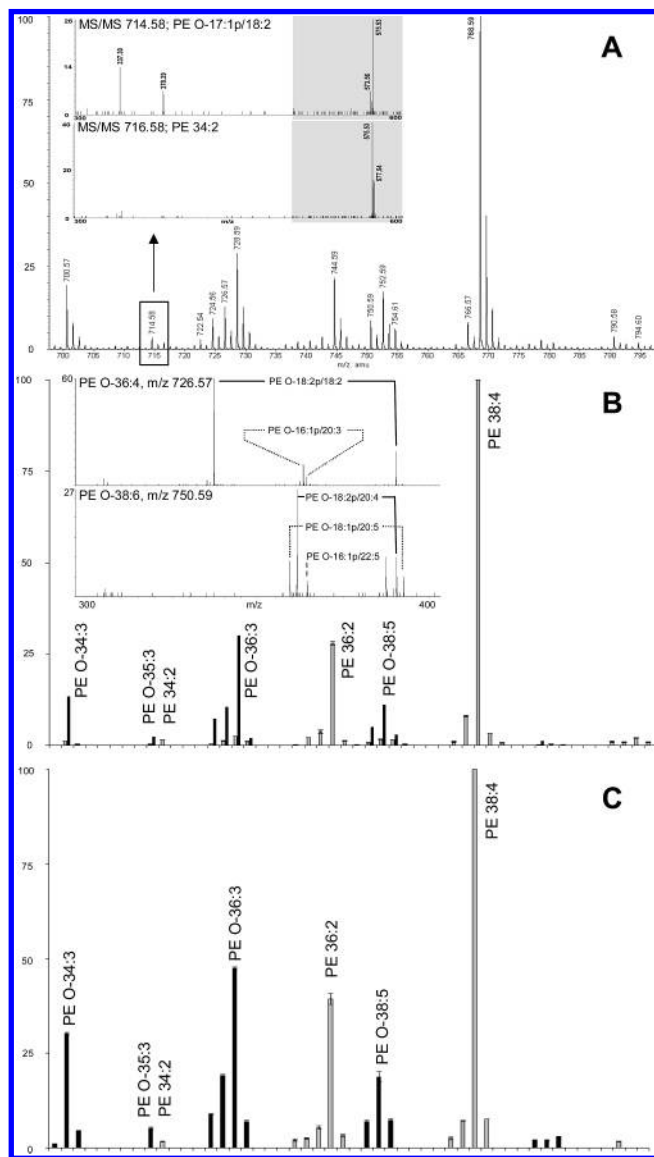


**Figure 5.** Profiling of PE species from bovine heart extract (total lipid concentration of 2.3 ng/ $\mu$ L) by +NLS  $\Delta m/z$  141.02 and Boolean plasmalogen-specific scans. (A) +TOF MS survey scan. Inset: tandem spectra acquired from  $m/z$  714.58 and 716.58 precursors. The spectra were combined from two MS/MS periods performed as described in the text. The highlighted  $m/z$  ranges were acquired under the low Q1 resolution settings for emulating the neutral loss profile. (B) Normalized profile of PE species determined by DDA-driven NLS  $\Delta m/z$  141.02 (shaded bars). Normalized profile of PE plasmalogens (filled bars) was determined by the Boolean scan that considered  $m/z$  of plasmalogen-specific fragment ions that are characteristic to 1-*O*-alk-1'-enyl 2-acyl moieties. Inset: parts of tandem mass spectra acquired from the precursor ions with  $m/z$  726.57 and 750.59 presenting the characteristic fragments, dissecting the structure of individual isobaric plasmalogen species. (C) Normalized PE profiles determined by FAS method in the negative ion mode. Filled bars, the identified plasmalogen species; shaded bars, PE species.

enabled recognition of lipids with ether bonds in parallel with lipid class specific profiling.

We analyzed a sample of bovine brain PEs by +TOF MS (Figure 5A) and by DDA-driven +NLS  $\Delta m/z$  141.02 (Figure 5B). PE species were identified, their peak areas normalized to the area of the most abundant peak (shaded bars in panels B and C Figure 5). We then used exact  $m/z$  of neutral loss  $\Delta m/z$  141.02

products to calculate the composition of moieties attached to the glycerol backbone. In several instances, the accurate values of  $m/z$  indicated that these precursors should comprise one ether and one ester, rather than two ester, bonds (shaded bars in Figure 5B). To confirm these assignments, the same sample was profiled by FAS in the negative ion mode (Figure 5C). FAS revealed that, in contrast to diacyl PE species, only one acyl anion of the fatty acid moiety was detectable for each of these plausible ether precursors, thus suggesting that a 1-*O*-alkyl or 1-*O*-alk-1'-enyl group was located at the *sn*-1 position at their glycerol backbone. Importantly, both methods—FAS and DDA-driven +NLS  $\Delta m/z$  141.02 with accurate measurement of fragment  $m/z$ —independently identified exactly the same pool of ether species.

In another project presented below, by taking advantage of high mass accuracy, neutral loss scanning was able to distinguish, within the same lipid class, isobaric species with seven double bonds and saturated species short by one methylene group whose masses differed by 0.0939 Da ( $M_{H_{12}} - M_C$ ). Similarly, ether species with seven double bonds were distinguishable from ester species short by two methylene groups and having a mass difference of 0.0575 Da ( $M_{H_{50}} - M_{C_2}$ ). We note, however, that although the mass resolution of Q(q)TOF instrument ( $\sim 10\,000$  fwhm) enabled us to confirm the identification of species, it might not allow a unequivocal resolution of the corresponding peaks would they be simultaneously present. Computer simulations suggested that a mass resolution of at least 30 000 is required, which is now attainable on a new generation of hybrid mass spectrometers with Fourier Transform (FT) mass analyzers.

**Boolean Scans: Accurate Identification of Plasmalogen Species.** Software-assisted processing of the entire body of MS/MS data enabled the identification of spectra, which contain fragments whose  $m/z$  met several selection criteria bundled by Boolean logical operators. Such Boolean scans can be performed in parallel with emulating conventional precursor or neutral loss scanning and would be impossible within conventional analytical approaches. Here, we applied Boolean scans to identify and quantify PE plasmalogen species in the same preparation of PEs from bovine heart.

Although ether species were identified by neutral loss scanning, it was not possible to tell whether they belonged to 1-*O*-alkyl or 1-*O*-alk-1'-enyl classes. Furthermore, plasmalogens are typically underrepresented in conventional +NLS  $\Delta m/z$  141.02 scans because of much less efficient neutral loss of the headgroup, compared to diacyl PEs or PEs with an alkyl moiety at the *sn*-1 position.<sup>37</sup> However, the MS/MS spectrum acquired from a low-abundant prospective plasmalogen precursor,  $m/z$  714.58, revealed two fragment ions specifically determining the moieties at *sn*-1 ( $m/z$  378.29) and *sn*-2 ( $m/z$  337.30) positions, respectively,<sup>37</sup> along with the minor peak of a neutral loss 141.02 fragment at  $m/z$  573.56. Because of the low resolution of the Q1 quadrupole, a neighboring precursor PE 34:2 was partially co-selected and, upon its collision-induced fragmentation, produced the abundant neutral loss fragment at  $m/z$  575.53 (insets in panel A of Figure 5).

Using  $m/z$  of position-specific fragments in MS/MS spectra of plasmalogens, we set up a Boolean scan to identify and quantify them in unseparated mixtures with other lipids, which was

(37) Zemski Berry, K. A.; Murphy, R. C. *J. Am. Soc. Mass Spectrom.* **2004**, *15*, 1499–1508.

implemented as an option in LipidInspector software. To be recognized as a plasmalogen, the fragmented precursor was required to meet the following criteria, which was equivalent to matching a set of arithmetic inequalities bundled by the Boolean "AND" operator:

(a) The spectrum should contain a fragment ion with  $m/z$  corresponding to neutral loss of  $\Delta m/z$  141.02 within the given mass tolerance (typically, 0.05 Da).

(b) Within the specified  $m/z$  range (typically, 250–450 Da), the spectrum should contain a complementary pair of fragments whose sum of  $m/z$  matched the  $m/z$  of the protonated precursor plus 1 Da within the given mass tolerance (typically, 0.05 Da).

(c) The nominal  $m/z$  of one of these fragments should be even (loss of a neutral fragment containing the fatty acid ester), whereas the nominal  $m/z$  of another fragment should be odd (loss of a neutral fragment containing the headgroup and the vinyl alcohol).<sup>37</sup>

(d) The intensity of these fragments should differ by a factor of 3 within the certain tolerance (typically,  $\pm 25\%$ ).

This Boolean plasmalogen-specific scan was applied to a full dataset of tandem mass spectra and identified all ether species as plasmalogens (the two examples of corresponding tandem mass spectra are presented in the inset in Figure 5B). When several isobaric plasmalogen species were present,  $m/z$  726.6 (PE O-16:1p/20:3 and PE O-18:2p/18:2) 750.6 (PE O-18:1p/20:5, PE O-18:2p/20:4, PE O-16:1p/22:5), they were correctly identified and individual molecular species reported. The results of DDA-driven Boolean profiling were in good agreement with both FAS identifications and neutral loss identifications of ether species described above.

To test whether the plasmalogen profile detected by DDA was also in quantitative agreement with FAS, we summed up the intensities of plasmalogen-specific ions and normalized the sums to the intensity of the most abundant peak in the +NLS  $\Delta m/z$  141.02 scan, to display both PEs and plasmalogens on the same scale (shaded bars at the panel B Figure 5). We then did similar normalization for FAS profiles, using the +TOF MS spectrum as a reference (shaded bars in panel C, Figure 5). Although the absolute quantities of PEs and plasmalogens could not be inferred, we noted that the profiles acquired by both FAS and DDA-driven scans followed the profile determined by +TOF MS, which should be expected for a relatively pure standard mixture. The identified plasmalogen and PE species, and their relative abundance determined by both approaches, also agreed well. Thus, we concluded that Boolean scans, a novel analytical feature of DDA-driven profiling, is a valid approach for identifying and quantifying molecular species of lipids.

**Profiling of Triacylglycerols by DDA-Driven Multiple Neutral Loss Scanning.** Although neutral TAGs and diacylglycerols are not protonated under the typical conditions of electrospray analysis, they can be detected in the positive ion mode as lithium or ammonium adducts. Collision-induced dissociation of lithium adducts results in neutral loss of the fatty acid moieties from all three positions of the glycerol backbone, yielding corresponding diacyl glycerol cations.<sup>22,38</sup> Han and Gross profiled an unseparated TAG mixture by consecutive neutral loss scans

using masses of acyl moieties of a few most common fatty acids.<sup>22</sup> Since DDA-driven profiling could emulate parallel (rather than consecutive) acquisition of a large number of neutral loss scans, we reasoned that it could greatly simplify the analysis of the molecular composition of complex mixtures of endogenous TAGs, with no recourse to any preliminary knowledge of their fatty acid composition.

Total lipid extract of *C. elegans* worms was separated by preparative TLC. The band containing TAGs was scraped, extracted using the modified method of Folch et al.,<sup>34</sup> and subjected to mass spectrometric analysis. Figure 6A presents the +TOF MS spectrum of the isolated fraction. The extract was then subjected to DDA-driven profiling. To accurately resolve the neighboring species, Q1 was operated under the unit mass resolution settings. The subsequent automated interpretation of the dataset by the LipidInspector was equivalent to the parallel acquisition of 69 neutral loss spectra relevant to losses of ammonia and fatty acids comprising 9 to 22 carbon atoms and zero to six double bonds. In each MS/MS spectrum, the corresponding neutral loss fragments were identified and their intensities summed up and normalized (Figure 6B). The relative intensities of the corresponding TAG species, which were designated by the total number of carbon atoms and double bonds in their three fatty acid moieties, agreed well with +TOF MS spectrum in Figure 6A and, in total, recognized 35 TAGs with the unique sum formula.

The acquired MS/MS spectra indicated that the molecular composition of TAGs was very heterogeneous, with each precursor ion representing 5 to 15 isobaric species. We further estimated the relative abundance of species with the unique fatty acid composition, although their positional isomers (i.e., TAGs, having the same fatty acid composition, but differing by their relative position at the glycerol backbone), were not distinguished. MS/MS fragmentation of a few synthetic TAG standards suggested that the relative abundance of the fragment rendered by the loss of the fatty acid from the *sn*-2 position is  $\sim 60\%$  of the abundance of the fragment rendered by the loss from the *sn*-1 position and is relatively independent of the fatty acid moiety (data not shown). To simplify the quantitative interpretation of spectra, we assumed that the yield of neutral loss products is approximately independent of the fatty acid and its position at the backbone. Considering the relative intensities of detected neutral loss fragments, we composed a system of linear equations for each fragmented precursor and calculated the relative abundance of species with the unique fatty acid composition. Details of the calculations and the estimate of their accuracy are provided in Supporting Information. The molecular composition of three isobaric lipids, TAG 49:2, TAG 51:3, and TAG 53:3, and the approximate estimate of the relative abundance of individual species are presented in Figure 6C. We note here that MS<sup>3</sup> fragmentation on an ion trap mass spectrometer provides an alternative approach to deciphering the molecular composition of TAGs.<sup>38</sup> However, DDA-driven analysis can be performed in parallel with the identification and quantification of other species and, since it solely relies on MS<sup>2</sup> (rather than MS<sup>3</sup>) fragmentation, attains the sensitivity at the nanomolar range of the concentration of lipid analytes (Table 1).

**Profiling of Total Lipid Extracts by DDA-Driven Multiple Neutral Loss and Precursor Ion Scanning.** Previous experiments were performed on lipid mixtures, which, albeit having

(38) McAnoy, A. M.; Wu, C. C.; Murphy, R. C. *J. Am. Soc. Mass Spectrom.* 2005, 16, 1498–1509.



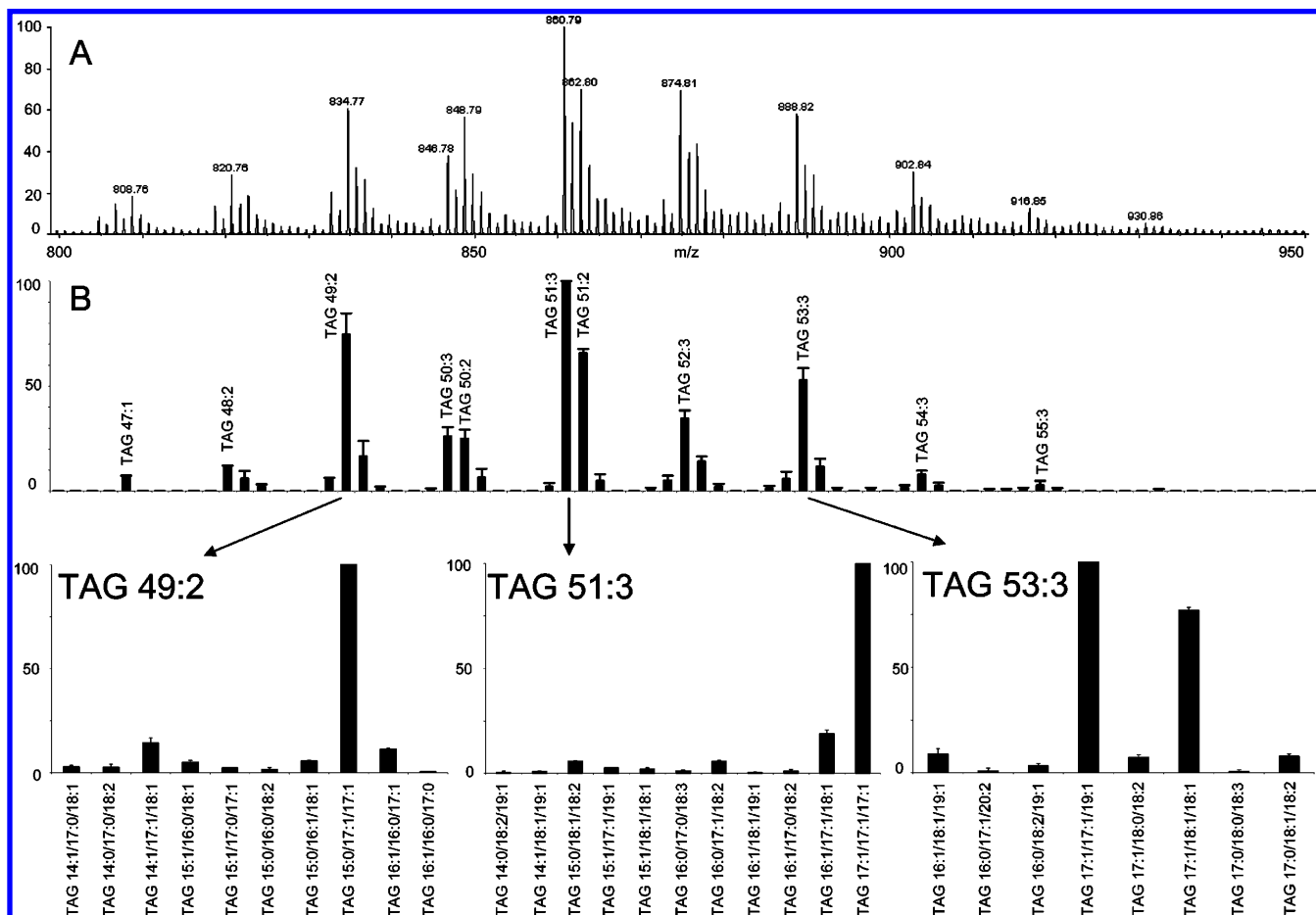


**Figure 6.** Profiling of the TAGs fraction isolated from the total *C. elegans* extract by preparative TLC. (A) +TOF MS survey scan. (B) Normalized profile of TAGs determined by DDA-driven emulation of 69 neutral loss scans specific for common fatty acid moieties. (C) Relative quantification of isobaric TAGs. Calculation details are presented in Supporting Information. The average error for calculated relative abundances of species was estimated in two independent experiments: 12% for TAG 49:2, 6% for TAG 51:3, and 14% for TAG 53:3. To calculate the relative abundances, systems of 11 linear equations for 10 species (TAG 49:2), 13 equations for 11 species (TAG 51:3), and 11 equations for 9 species were solved.

complex molecular compositions, only contained lipids of the same class. We next tested whether DDA-driven profiling could simultaneously identify and quantify lipids of multiple classes from a total unseparated extract. Lipids were extracted from *C. elegans* worms, and the total extract was directly infused into a Q(q)TOF mass spectrometer and subjected to DDA-driven profiling, as described above. The acquired pool of tandem mass spectra was interpreted by the LipidInspector providing three neutral loss scans, one precursor ion scan, and one Boolean plasmalogen-specific scan, and the intensities of identified species were normalized (Figure 7). As anticipated, PEs and PCs accounted for the major peaks detected by +TOF MS (Figure 7A–C). Interestingly, the major PE-plasmalogen species (PE O-18:1p/18:1) was identified at  $m/z$  730.58, while at  $m/z$  732.58 +NLS  $\Delta m/z$  141.02, together with the accurate mass measurement of the neutral loss fragment, identified the ether lipid PE O-36:1. With the exception of another two plasmalogen (but not ether) species, other peaks detectable at +NLS  $\Delta m/z$  141.02 were diacyl PEs. This clearly underscores that +NLS  $\Delta m/z$  141.02 alone lacks the required specificity for accurate profiling of various classes of PEs.<sup>37</sup> The peaks at  $m/z$  820.74 and 822.74 were identified as ammonia adducts of TAG 48:2 and TAG 48:1, although the bulk of extractable TAGs was detected at the higher  $m/z$  range and is not presented in Figure 7. The identification of several highly unsaturated PCs by +PIS

$\Delta m/z$  184.07 was supported by the accurate mass measurement of the precursors, as described above, which clearly differentiated them from isobaric species with a fatty acid moiety having an odd number of carbon atoms. Similar species with polyunsaturated fatty acid moieties were previously observed in *C. elegans* lipid extracts by Tanaka et al.<sup>39</sup> and most likely comprised 20:5 and 20:4 fatty acids. Altogether, DDA-driven identification recognized 90 glycerophospholipids with the unique molecular composition and provided their relative (within a given class) quantification in a single direct infusion experiment. Since the detection and quantification of lipids relied on specific precursor and neutral loss scans, spiking the appropriate internal standard(s)<sup>2,25</sup> into the analyte would be required for their absolute quantification. To dissect the molecular composition of glycerophospholipids by precisely identifying their fatty acid moieties, the same sample could be further analyzed by FAS in the negative ion mode as described previously.<sup>3,27</sup> Alternatively, DDA-driven experiments could be set up such that the acyl anions of fatty acids could be determined from MS/MS spectra and assigned to the corresponding lipid species by considering  $m/z$  of fragmented precursors.

Thus, we demonstrated that complex lipid mixtures are amenable to the DDA-driven characterization, which also provides

(39) Tanaka, T.; Izuwa, S.; Tanaka, K.; Yamamoto, D.; Takimoto, T.; Matsuura, F.; Satouchi, K. *Eur. J. Biochem.* **1999**, *263*, 189–195.

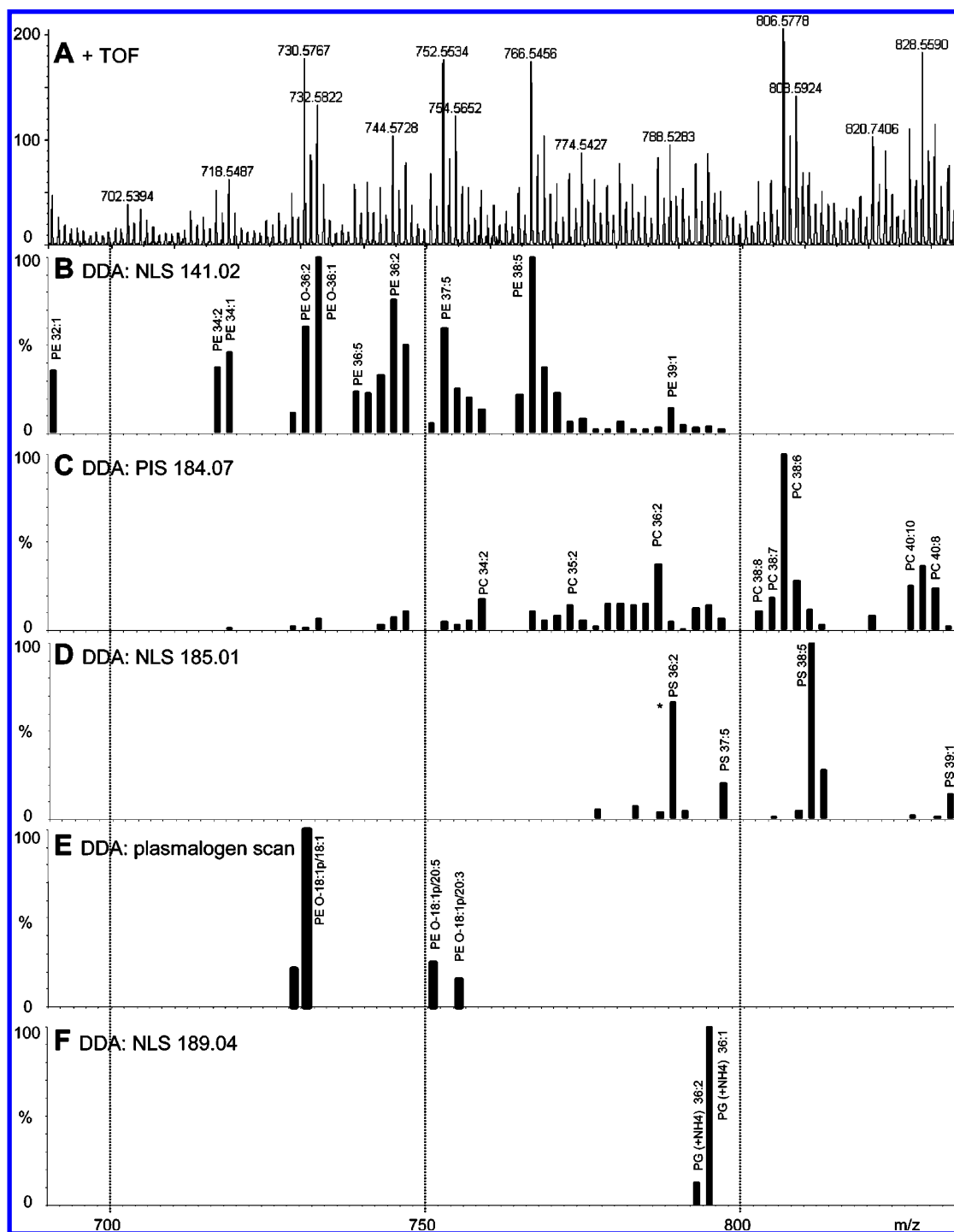


**Figure 7.** DDA-driven profiling of the total lipid extract of *C. elegans*. Data for all profiles were acquired in parallel. (A) +TOF MS survey scan; (B) normalized profile of PEs determined by DDA-driven +NLS  $\Delta m/z$  141.02; (C) normalized profile of PCs determined by DDA-driven +PIS  $m/z$  184.07; (D) normalized profile of PSs determined by DDA-driven +NLS  $\Delta m/z$  185.01, the internal standard PS 36:2 is designated with the asterisk; (E) normalized profile of PE plasmalogens determined by the plasmalogen-specific DDA-driven scanning; (F) normalized profile of ammonium adducts of PGs determined by DDA-driven +NLS  $\Delta m/z$  189.04.

more specific information on the identity of lipid species, compared to conventional precursor and neutral loss scans.

## CONCLUSION AND PERSPECTIVES

DDA-driven lipid profiling capitalizes on the high-end capabilities of Q(q)TOF instruments, such as the high mass resolution, mass accuracy, and acquisition speed, both in MS and in MS/

MS modes, together with the accurate selection of precursors. Although we solely used a Q(q)TOF in this work, the above features are also offered by a new generation of high-resolution hybrid instruments, such as ion trap–FT ICR and the recently developed linear ion trap–orbitrap<sup>40</sup> mass spectrometers. Coupling of high-resolution mass analyzers with linear traps is especially promising because of their MS<sup>n</sup> capability, which is a powerful

tool in elucidating the molecular composition of various classes of lipids.<sup>3,38</sup> The interpretation of MS<sup>n</sup> fragmentation is often hampered by ion statistics; however, direct infusion of samples at the submicroliter per minute flow rate effectively leaves ample time for a series of in-depth fragmentation experiments.

DDA-driven profiling takes full advantage of the rich pattern of fragments observed in tandem mass spectra of lipids, whereas neutral loss scanning and precursor ion scanning (including multiple precursor ion scanning) rely on their very restricted subset. This opens up novel analytical opportunities, such as Boolean scans, in which many fragment ions are simultaneously considered within a single logical framework. We envision that, in the future, the software would be utilizing some kind of a meta language, in which the user could flexibly specify the interpretation rules such that the full body of acquired data could be reprocessed many times using alternative interpretation approaches.

In the presented experiments, we mostly used DDA that relied on inclusion lists. However, target precursors could also be determined automatically, followed by the acquisition of the full set of MS/MS data. This makes the DDA-driven approach a preferred tool in discovery projects, since there is no need to rely on the preliminary knowledge of the fragmentation pathways or expected characteristic fragments or neutral losses. Any kind of known fragmentation behavior would be automatically recognized,

(40) Hu, Q. Z.; Noll, R. J.; Li, H. Y.; Makarov, A.; Hardman, M.; Cooks, R. G. *J. Mass Spectrom.* **2005**, *40*, 430–443.

while preserving the spectra of unidentified species for subsequent in-depth interpretation.

Our results indicated that data-dependent acquisition and processing could become a powerful tool in lipidomics, expanding a limited palette of mass spectrometric methods currently available in the field.

#### ACKNOWLEDGMENT

We are grateful to Prof. Kai Simons (MPI CBG) for useful discussions on the lipidomic strategies; Dr. Igor Chernushevich (MDS Sciex) for expert advice on quadrupole time-of-flight mass spectrometry; to members of Shevchenko laboratory for their expert support; and Ms. Judith Nicholls (MPI CBG) and Dr. Michaela Scigelova (ThermoElectron Corp., San Jose CA) for critical reading of the manuscript. This project was funded in part by SFB/TR 13 grant from Deutsche Forschungsgemeinschaft to A.S. (project D1) and T.K. (project B2).

#### SUPPORTING INFORMATION AVAILABLE

Additional information as noted in text. This material is available free of charge via the Internet at <http://pubs.acs.org>.

Received for review September 8, 2005. Accepted November 1, 2005.

AC051605M